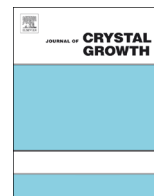




ELSEVIER

Contents lists available at [SciVerse ScienceDirect](http://www.sciencedirect.com)

## Journal of Crystal Growth

journal homepage: [www.elsevier.com/locate/jcrysgr](http://www.elsevier.com/locate/jcrysgr)

## Cubic GaN quantum dots embedded in zinc-blende AlN microdisks



M. Bürger\*, R.M. Kemper, C.A. Bader, M. Ruth, S. Declair, C. Meier, J. Förstner, D.J. As

University of Paderborn, Department of Physics, Warburger Str. 100, 33098 Paderborn, Germany

## ARTICLE INFO

Available online 3 January 2013

## Keywords:

A1. Etching  
 A1. Low dimensional structures  
 A1. Nanostructures  
 A1. Optical microscopy  
 A3. Molecular beam epitaxy  
 B1. Nitrides

## ABSTRACT

Microresonators containing quantum dots find application in devices like single photon emitters for quantum information technology as well as low threshold laser devices. We demonstrate the fabrication of 60 nm thin zinc-blende AlN microdisks including cubic GaN quantum dots using dry chemical etching techniques. Scanning electron microscopy analysis reveals the morphology with smooth surfaces of the microdisks. Micro-photoluminescence measurements exhibit optically active quantum dots. Furthermore this is the first report of resonator modes in the emission spectrum of a cubic AlN microdisk.

© 2012 Elsevier B.V. All rights reserved.

## 1. Introduction

In the early 1990s semiconductor microdisks were first proposed as lasing devices [1]. Since their introduction many efforts were made to fabricate microdisk lasers with high quality factors  $Q$  ( $Q$ -factors) to reduce laser thresholds [2]. In contrast to other photonic resonators (e.g. photonic crystal nanocavities) the fabrication of microdisks is relatively straight forward. Due to internal total reflection of the whispering gallery modes (WGM) microdisks feature a strong confinement. Up to now microdisks of many materials were realized but in case of group III-nitrides only microdisks of wurtzite AlN/GaN were fabricated [3,4]. However, hexagonal GaN built-in electric fields induce a Quantum Confined Stark Effect. As a consequence the recombination probability of electrons and holes is reduced, what is undesirable for optical devices. To avoid these internal spontaneous polarization fields group III-nitrides can be grown in the meta-stable cubic phase in (0 0 1) growth direction [5]. Hence cubic wide-bandgap group III-nitrides (c-GaN, c-AlN) are promising materials for future quantum optical devices with applications in photonics and quantum information processing.

Very recently the possibility of producing optical devices from non-polar nitrides arised by depositing c-AlN layers confining c-GaN quantum dots (QDs) [6,7]. To improve the light extraction efficiency QDs can be integrated into microresonators (e.g. microdisks). Compared to quantum wells QDs have the advantage of reducing optical losses in the active region due to lower absorption. QDs embedded into microresonators would thereby be suitable for devices like solid-state based single photon emitters

for quantum information technology as well as low threshold laser devices.

This work reports on the growth of c-AlN confinement layers and c-GaN QDs via plasma assisted molecular beam epitaxy (PAMBE) [6]. We fabricated microdisks of our structures by two sequenced dry chemical etching steps. The morphology of free-standing mushroom shaped microdisk structures was investigated by scanning electron microscopy (SEM). Furthermore we performed micro-photoluminescence ( $\mu$ -PL) spectroscopy measurements to characterize the microdisks optical properties.

## 2. Experiment

Our cubic group III-nitride samples were grown on 10  $\mu$ m 3C-SiC on top of a Si (0 0 1) substrate using a Riber 32 MBE system with standard Ga and Al effusion cells and an Oxford Instruments N plasma source. The growth process was *in situ* controlled by means of reflection high energy electron diffraction (RHEED) [8]. The grown structure consists of a single layer c-GaN QDs sandwiched between two 30 nm c-AlN barrier layers.

Structuring of the microdisks began with the deposition of a 80 nm SiO<sub>2</sub> etching mask using plasma enhanced chemical vapor deposition. Electron beam lithography was used to define microdisks of various diameters (i.e. 2–8  $\mu$ m). The SiO<sub>2</sub> mask was etched by reactive ion etching (RIE) using CHF<sub>3</sub> and Ar. For transferring the pattern into the structure the samples were etched by anisotropic RIE by means of SiCl<sub>4</sub> and Ar chemistry in an Oxford Plasmalab 100 etching system. Afterwards the SiO<sub>2</sub> mask was removed from the circular pillars by buffered oxide etching solution (BOE). The undercut of the active layer was realized by selective dry etching of the 3C-SiC substrate. An etching process for a microdisk consisting of a c-AlN/GaN slab on a 3C-SiC post must be selective to group III-nitrides. For that

\* Corresponding author. Tel.: +49 5251605831; fax: +49 5251605843.  
 E-mail address: mbuerger@mail.uni-paderborn.de (M. Bürger).

purpose tetrafluoromethane ( $\text{CF}_4$ ) is introduced at a temperature of  $375^\circ\text{C}$  in an additional Oxford Plasmalab 100 etching system including a heated sample holder. Lateral etching of 3C-SiC requires further input of thermal energy to the substrate. The substrate temperature is the crucial factor for isotropic etching of 3C-SiC in order to activate the chemical reaction [9]. Due to its excellent mechanical and chemical stability, a feasible wet chemical etching technique like in GaAs and Si processing is not available for epitaxial 3C-SiC [10].

We performed the optical microdisk characterization by a confocal  $\mu$ -PL setup. As excitation source, a 325 nm HeCd Laser with an excitation power of 17 mW was used. An UV-microscope objective ( $80\times$ ,  $\text{NA}=0.55$ ) focused the laser beam into a diffraction limited spot of approximately 720 nm diameter ( $d\sim 1.22\lambda/\text{NA}$ ). PL spectra were collected at low temperature using a 0.5 m Princeton Instruments grating monochromator and a UV-enhanced charge-coupled device. A piezo  $xy$ -stage with a driving accuracy of 50 nm inside a liquid He cooled cryostat enables spatially resolved low temperature PL measurements.

### 3. Results and discussion

The sample fabrication started with the growth of a 30 nm AlN buffer layer at  $760^\circ\text{C}$  substrate temperature. The RHEED pattern of the buffer layer taken in  $[1\ 1\ 0]$  azimuth (Fig. 1(a)) shows long thin streaks indicating a smooth two-dimensional surface [11]. Due to the lattice mismatch of 3.2% between c-GaN and c-AlN QDs can be created by the well known Stranski Krastanov (SK) growth process [7]. The QD formation occurs after the deposition of a two monolayer (ML) thick c-GaN layer (critical thickness) on c-AlN. The QD density and size can thereby be controlled by the amount of deposited GaN [6]. The RHEED pattern in Fig. 1(b) features spotty reflections revealing three dimensional islands of cubic crystal structure after introducing the QD formation. Typical QD densities of uncapped samples were obtained in former studies by atomic force microscopy and are in the order of  $10^{11}\text{ cm}^{-2}$  [12].

To cover the c-GaN QDs a 30 nm c-AlN cap layer was grown at a substrate temperature of  $760^\circ\text{C}$ . The RHEED pattern in Fig. 1(c) shows long thin streaks without spotty reflections indicating again a smooth c-AlN surface and a complete overgrowth of the QDs.

Fig. 2(a) shows a side view SEM image of an undercut microdisk with a diameter of  $2.5\ \mu\text{m}$ . No bowing of the 60 nm thick slab is apparent, although the different layers are slightly strained. To make sure that the active layer was interpenetrated the first etching depth was extended to 100 nm. The 3C-SiC post

exhibits an etching step. During 3C-SiC etching a fluorocarbon film from the etching product species is deposited on the pedestal sidewalls [13]. This passivation layer inhibits the chemical etching rates. The disk acts as a mask and prevents the removal of the layer by ion bombarding on the pedestal sidewalls. Due to the clear undercut the chemical etching process seems to dominate on the backside towards the disk center. A closer view on the sidewalls in Fig. 2(b) reveals little vertical striations and a slightly sloped sidewall. We ascribe the imperfect sidewalls to mask erosion during the first dry etching process. The top down view of the microdisk illustrates its circularity (Fig. 2(c)). Additionally contrast differences in the center of the microdisk indicate the double step 3C-SiC post. The 3C-SiC post is approximately square shaped due to the selective etching properties of the  $\text{CF}_4$  dry etching in the  $[1\ 1\ 0]$  and  $[-1\ 1\ 0]$  crystal orientation.

Fig. 3 shows PL spectra taken at 11 K of an unstructured sample (grey line) and a  $2.5\ \mu\text{m}$  diameter microdisk (black line). A broad luminescence band with a full width at half maximum (FWHM) of 0.17 eV at about 3.58 eV was observed in the reference spectrum. This emission band is related to the QD ensemble luminescence [14]. The confinement energy of the QDs leads to a larger transition energy compared to the band gap energy of bulk c-GaN [15]. The PL-spectrum of a single QD has a very narrow FWHM compared to a spectrum of GaN bulk material. Hence the ensemble luminescence is a superposition of many single QD emission lines and the emission band is correlated to the size distribution of the QDs [16].

The black spectrum shows luminescence from a  $2.5\ \mu\text{m}$  diameter microdisk containing QDs. The luminescence band centered at 3.59 eV with a FWHM of 0.17 eV is associated with the emission of the QD ensemble. If the QD emission couples to resonant modes of the microdisk, the luminescence intensity can be increased. In this spectrum additional separated peaks appear. These peaks are announced in terms of WGMs of the microdisk. Different radial order modes can be assumed in the periphery of the microdisk. The radial mode number is denoted by  $l=1, 2, \dots$ . We attributed the additional peaks to the first ( $l=1$ ) and second order ( $l=2$ ) of WGMs. For the mode at 3.55 eV a  $Q$ -factor of 400 can be estimated. The spectral mode spacing, named the free spectral range (FSR), is for the first order modes about  $\Delta E_1=72\text{ meV}$  and for the second order modes about  $\Delta E_2=78\text{ meV}$  in the range of 3.6 eV (indicated by vertical arrows). Higher ordered modes exhibit larger mode spacing than lower ordered modes [17]. Fabry-Pérot layer oscillations of the  $10\ \mu\text{m}$  3C-SiC substrate can be neglected, since the disk is surrounded by air. Layer oscillations in growth direction of the 60 nm slab would exhibit a large period of  $\Delta E=4.6\text{ eV}$  and receive thereby no consideration. Three dimensional finite difference time domain (FDTD) calculations were carried out to determine

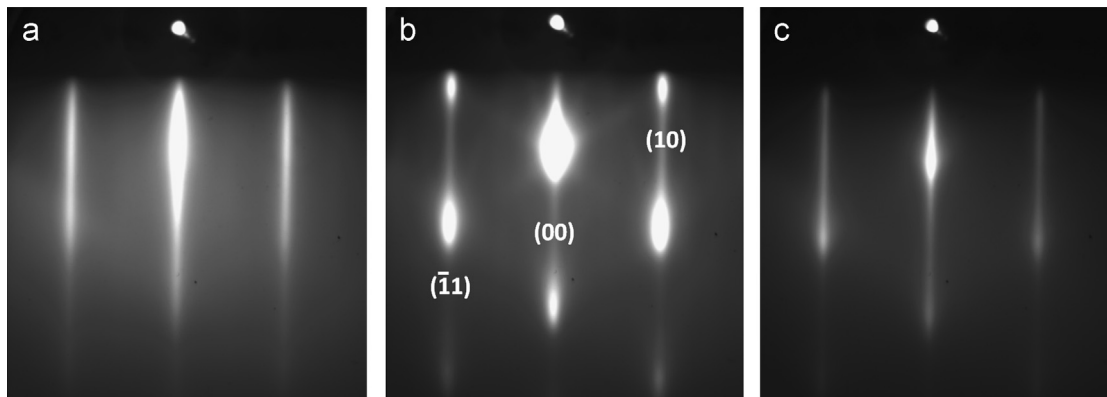
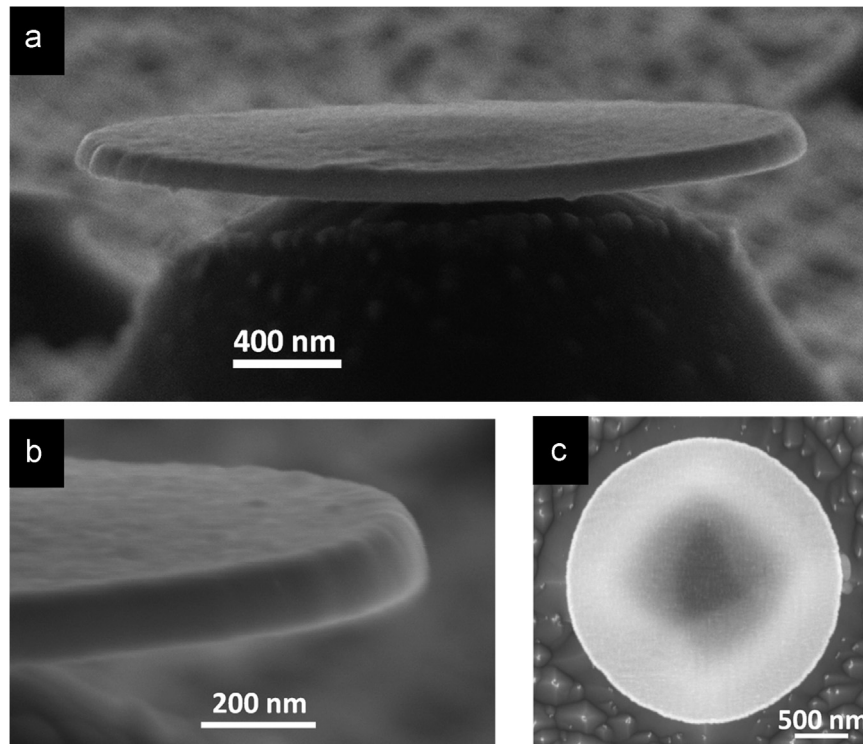
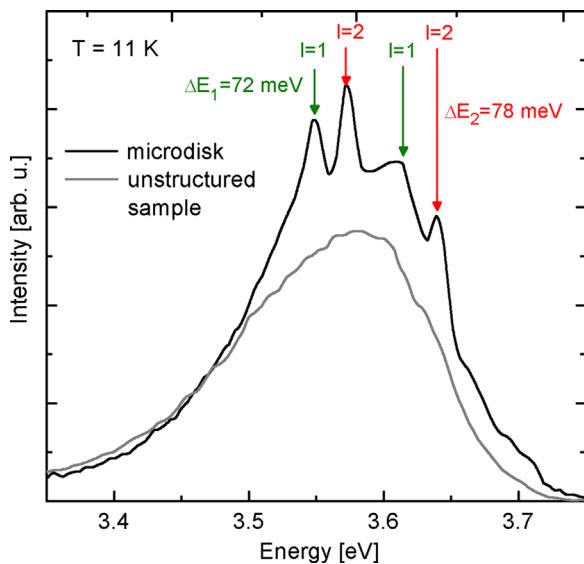


Fig. 1. RHEED patterns: (a) reflections of the c-AlN buffer layer, long thin streaks indicate a smooth two-dimensional surface, (b) reflections of c-GaN SK QDs, the spotty reflections indicate three dimensional islands of cubic crystal structure, (c) reflections of the c-AlN cap layer after 30 ML QD overgrowth.



**Fig. 2.** SEM images of a c-AlN microdisk with a diameter of 2.5  $\mu\text{m}$  fabricated by RIE etching. (a) Side view of the microdisk. (b) Close up view of the sidewall. (c) Top down view of the microdisk.



**Fig. 3.** PL-spectrum of c-GaN QDs embedded in a 2.5  $\mu\text{m}$  diameter c-AlN microdisk (black line) and an unstructured sample as reference (grey line). The mode spacing of the first two families of radial modes are indicated by vertical arrows.

the FSR [18]. Detailed information of the FDTD calculations will be given elsewhere. A good agreement between the experimental results and the calculated FSR as well as the exclusion of Fabry–Pérot layer oscillations confirms our interpretation of the observed additional peaks as WGMs.

Whispering gallery modes in hexagonal AlN microdisks with 2  $\mu\text{m}$  diameter which contain hexagonal GaN QDs showed  $Q$ -factors up to 5000 [19]. Imperfections of disk sidewalls and surfaces as well as the crystal quality of the c-AlN layers may influence the propagating wave and reduce the  $Q$ -factor in our

case. Due to the relatively low observed  $Q$  values a weak coupling between the active region and the resonator modes can be concluded. Scattering processes in the microdisk and at the sidewall roughness leads to optical loss mechanisms.

#### 4. Conclusion

We have developed a process to fabricate reliably undercut microdisks of meta-stable cubic group III-nitrides. The active layer consists of two 30 nm thick c-AlN confinement layers containing a single layer of c-GaN QDs. Our disks were patterned by electron beam lithography. The morphological investigation by SEM shows good circularity and low sidewall roughness of the microdisks. Micro-PL spectroscopy reveals optically active QDs in the microdisk at low temperature. Resonator modes of the two first radial orders were observed. These are the first steps towards an investigation of microdisks featuring modes with high  $Q$ -factors and lasing properties.

#### Acknowledgments

This work was supported by the DFG graduate program GRK 1464 “Micro- and Nanostructures in Optoelectronics and Photonics”. K. Lischka and T. Schupp and are acknowledged for helpful discussions.

#### References

- [1] S.L. McCall, A.F.J. Levi, R.E. Slusher, S.J. Pearson, R.A. Logan, *Applied Physics Letters* 60 (1992) 289.
- [2] A. Pawlis, M. Panfilova, D.J. As, K. Lischka, K. Sanaka, T.D. Ladd, Y. Yamamoto, *Physical Review B* 77 (2008) 153304.
- [3] H.W. Choi, K.N. Hui, P.T. Lai, P. Chen, X.H. Zhang, *Applied Physics Letters* 89 (2006) 211101.

- [4] E.D. Haberer, R. Sharma, C. Meier, A.R. Stonas, S. Nakamura, S.P. DenBaars, E.L. Hu, *Applied Physics Letters* 85 (2004) 5179.
- [5] D.J. As, *Microelectronics Journal* 40 (2009) 204.
- [6] T. Schupp, K. Lischka, D.J. As, *Journal of Crystal Growth* 312 (2010) 3235.
- [7] T. Schupp, T. Meisch, B. Neuschl, M. Feneberg, K. Thonke, K. Lischka, D.J. As, *AIP Conference Proceedings* 1292 (2010) 165.
- [8] J. Schörmann, S. Potthast, D.J. As, K. Lischka, *Applied Physics Letters* 90 (2007) 041918.
- [9] F. Niebelschutz, J. Pezoldt, T. Stauden, V. Cimalla, K. Tonisch, K. Bruckner, M. Hein, O. Ambacher, A. Schober, *IEEE Electronics Devices* 43 (1996) 1732.
- [10] D. Zhuang, J.H. Edgar, *Materials Science and Engineering R* 48 (2005) 1–46.
- [11] W. Braun, *Applied RHEED*, Springer Tracts in Modern Physics, vol. 154, Springer, Berlin, 1999.
- [12] M. Bürger, T. Schupp, K. Lischka, D.J. As, *Physica Status Solidi (c)* 9 (5) (2012) 1273.
- [13] D.C. Gray, V. Mohindra, H.H. Sawin, *Journal of Vacuum Science and Technology A* 12 (1994) 354.
- [14] T. Schupp, K. Lischka, D.J. As, *Journal of Crystal Growth* 323 (2011) 286.
- [15] D.J. As, F. Schmilgus, C. Wang, B. Schöttker, D. Schikora, K. Lischka, *Applied Physics Letters* 70 (1997) 1311.
- [16] G. Schmid, *Nanoparticles: From Theory to Application*, Wiley-VCH, New York, 2006.
- [17] M. Borselli, T.J. Johnson, O. Painter, *Optics Express* 13 (2005) 1515.
- [18] S. Declair, C. Meier, T. Meier, J. Förstner, *Photonics and Nanostructures – Fundamentals and Applications* 8 (2010) 273.
- [19] M. Mexis, S. Sergent, T. Guillet, C. Brimont, T. Bretagnon, B. Gil, F. Semond, M. Leroux, D. Néel, S. David, X. Chécoury, P. Boucaud, *Optics Letters* 36 (2011) 2203.